ORIGINAL ARTICLE

Characterization of development and artemisinin biosynthesis in self-pollinated *Artemisia annua* plants

Fatima Alejos-Gonzalez · Guosheng Qu · Li-Li Zhou · Carole H. Saravitz · Janet L. Shurtleff · De-Yu Xie

Abstract *Artemisia annua* L. is the only natural resource that produces artemisinin (Qinghaosu), an endoperoxide sesquiterpene lactone used in the artemisinin-combination therapy of malaria. The cross-hybridization properties of *A. annua* do not favor studying artemisinin biosynthesis. To overcome this problem, in this study, we report on selection of self-pollinated *A. annua* plants and characterize their development and artemisinin biosynthesis. Self-pollinated F2 plants selected were grown under optimized growth conditions, consisting of long day (16 h of light) and short day (9 h of light) exposures in a phytotron. The life cycles of these plants were approximately 3 months long, and final heights of 30–35 cm were achieved. The leaves on the main stems exhibited obvious morphological changes, from indented single leaves to odd, pinnately compound leaves. Leaves and flowers formed glandular and T-shaped trichomes on their surfaces. The glandular trichome densities increased from the bottom to the top leaves. High performance liquid chromatography–mass spectrometry-based metabolic profiling analyses showed that leaves, flowers, and young seedlings of F2 plants produced artemisinin. In leaves, the levels of artemisinin increased from the bottom to the top of the plants, showing a positive correlation to the density increase of glandular trichomes. RT-PCR analysis showed that progeny of self-pollinated plants expressed the amorpha-4, 11-diene

synthase (ADS) and cytochrome P450 monooxygenase 71 AV1 (CYP71AV1) genes, which are involved in artemisinin biosynthesis in leaves and flowers. The use of self-pollinated *A. annua* plants will be a valuable approach to the study of artemisinin biosynthesis.

Abbreviations

ADS	Amorpha-4, 11-diene
CYP71AV1	Cytochrome P450 monooxygenase 71 AV1
HPLC–ESI–MS	High performance liquid chromatography–electron spray ionization–mass spectrometry
MS	Murashige and Skoog
QHS	Qinghaosu

Introduction

Malaria is one of the most destructive parasitic diseases. More than one billion people worldwide have been exposed to malaria (WHO 2009a). In 2008, there were approximately 243 million cases of malaria and approximately 863,000 deaths worldwide (WHO 2009a). Most of the cases and deaths occurred in African countries. The most severe parasite is *Plasmodium falciparum*, which causes approximately 90% of malaria-infected deaths, particularly in children under 5 years old and in pregnant women (WHO 2009a). Currently, 77 (of 81) countries and territories are under the severe threat of *P. falciparum*

F. Alejos-Gonzalez · G. Qu · L.-L. Zhou · C. H. Saravitz · J. L. Shurtleff · D.-Y. Xie (✉)
Department of Plant Biology, North Carolina State University, Raleigh, NC 27695, USA
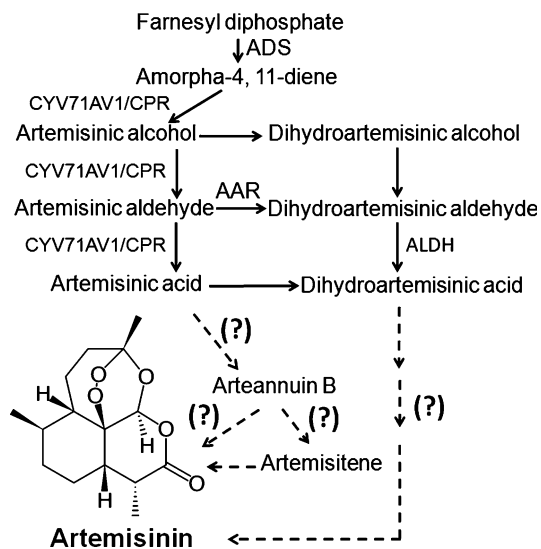e-mail: dxie@ncsu.edu

Fig. 1 Proposed biosynthetic pathway of artemisinin starting with farnesyl diphosphate. *AAR* artemisinic aldehyde reductase; *ADS* amorpha-4, 11-diene synthase; *ALDH* aldehyde dehydrogenase; *CYP71AV1* cytochrome P450 monooxygenase 71 AV1; *CPR*: NADPH: cytochrome P450 oxidoreductase

(WHO 2009b). Unfortunately, this parasite is resistant to antimalarial medicines, such as quinine and chloroquine. In addition, the parasite *P. vivax* is able to become resistant to chloroquine (WHO 2009c). Fortunately, artemisinin and its derivatives can be used to effectively cure malaria caused by these two parasites (WHO 2009b, 2010).

Artemisinin (Qinghaosu) (Fig. 1), an endoperoxide sesquiterpene lactone produced by *Artemisia annua*, is an effective antimalarial medicine (Liu et al. 1979; Tu et al. 1982; Zhong-Yi-Yan-Jiu-Yue-Zhong-Yao-Yan-Jiu-Suo 1978). Currently, the artemisinin-based combination therapy (ACT) is strongly recommended by the World Health Organization (WHO) to treat malaria particularly for the severe and cerebral malaria caused by the *P. falciparum* parasite (WHO 2009b, 2010). Consequently, the demand for artemisinin, which is mainly extracted from *A. annua*, has increased in recent few years. For example, in 2006, the number of individual treat courses of ACTs was approximately 85 million, and in 2007 and 2008, this number increased to approximately 95 million and 105 million, respectively (WHO 2009b). Furthermore, the 2009 World Malaria Report predicted that the production of artemisinin in 2010 would not meet this rapidly increasing demand (WHO 2009b).

A. annua is the only natural resource capable of producing artemisinin. Due to the low and variable contents of artemisinin in *A. annua*, the yield of this medicine cannot meet the increasing yearly demand for malarial treatments. To solve this problem, since the 1970s, substantial effort has been directed toward understanding the genetic characteristics of this plant and discovering or developing new

varieties with improved artemisinin production (Klayman et al. 1984; Liersch et al. 1986; Tu et al. 1982; WHO 1998, 2010). We previously reported that the karyotype of *A. annua* grown in Beijing was K (2n) = 18 = 12 m + 2sm + 3 m (SAT) + 2sm (SAT) (Xie et al. 1995) and this ecotype produced 0.1–0.5% of the artemisinin in dry leaves (Zhong-Yi-Yan-Jiu-Yue-Zhong-Yao-Yan-Jiu-Suo 1978). The artemisinin production of additional ecotypes of *A. annua* grown in different regions or countries has also been investigated (Delabays et al. 1993, 2001), revealing variable ranges from 0.01% to approximately 1.0% dry weight (Delabays et al. 2001; Ferreira et al. 2005). To increase artemisinin production, field growth protocols for genetic breeding were established for *A. annua* growth in different biogeographical territories (Delabays et al. 2001; Ferreira et al. 2005; WHO 2005, 2010), and a hybrid cultivar (Artemis) with a dry leaf artemisinin content of approximately 1.4% was obtained from a cross between an ecotype from China and an ecotype from Vietnam (Delabays et al. 2001). In 2010, new cultivars were reported to produce approximately 2.2% of artemisinin in their leaves (dry weight) (Smith et al. 2010). To understand artemisinin biosynthesis, a recent genetic map investigation of Artemis identified nine linkage groups associated with genetic variation and established a quantitative trait loci (QTL) map, showing key traits controlling artemisinin yields (Graham et al. 2010). This study will likely enhance the genetic breeding of *A. annua*.

Numerous methods have been discovered for characterizing the precursors of artemisinin and their biosynthesis. Starting with farnesyl diphosphate (FDP), a group of precursors have been biochemically identified, including amorpha-4, 11-diene, artemisinic alcohol, dihydroartemisinic alcohol, artemisinic aldehyde, dihydroartemisinic aldehyde, artemisinic acid, and dihydroartemisinic acid (Fig. 1) (Lommen et al. 2005, 2007; Wallaart et al. 1999; Wallaart et al. 2000). In addition, arteannuin B and artemisitene (Fig. 1) have been proposed to be two potential precursors (Acton and Klayman 1985; Lommen et al. 2005). Several key genes involved in the biosynthesis of these precursors have been cloned from *A. annua*. The amorpha-4, 11-diene synthase (ADS) gene was biochemically and transgenically demonstrated to encode the first committed enzyme in the artemisinin biosynthetic pathway starting with FDP (Fig. 1) (Bouwmeester et al. 1999; Chang et al. 2000; Covello et al. 2007; Martin et al. 2003; Mercke et al. 2000; Wallaart et al. 2001). The cloning and functional characterization of the cytochrome P450 monooxygenase 71 AV1 (CYP71AV1) gene and its partner, the NADPH: cytochrome P450 oxidoreductase gene, revealed the biosynthetic pathway of artemisinic acid (Ro et al. 2006; Teoh et al. 2006). The co-expression of *ADS*, *CYP71AV1*, and *CPR* in yeast led to the production of

artemisinic acid (AA) (Ro et al. 2006). Two genes, encoding an artemisinic aldehyde reductase (AAR, a double bond reductase) and an aldehyde dehydrogenase (ALDH), respectively, were cloned from *A. annua* (Teoh et al. 2009; Zhang et al. 2008). A recombinant AAR protein was shown to catalyze a reduction reaction converting artemisinic aldehyde to dihydroartemisinic aldehyde (Zhang et al. 2008). A recombinant ADH1 protein was shown to catalyze an NAD(P)-dependent oxidation converting dihydroartemisinic aldehyde to dihydroartemisinic acid (Teoh et al. 2009). In addition, a recent transgenic study showed that the co-expression of *ADS*, *CYP71AV1*, *AAR,* and *ADH1* in tobacco led to the formation of dihydroartemisinic alcohol (Zhang et al. 2010). These discoveries provided strong evidence on supporting this branch pathway, in which artemisinic alcohol is converted to dihydroartemisinic aldehyde (Fig. 1).

In comparison, little is understood regarding the genetic regulation of artemisinin biosynthesis in plants. Except for the naturally mutated glandless plant (Duke et al. 1994), there is no mutant evidence demonstrating the existence of any artemisinin biosynthetic pathways in plants. This is likely due to the cross-hybridization properties of *A. annua* (Delabays et al. 2001; Graham et al. 2010), which lead to massive variations of artemisinin biosynthesis in offspring plants and difficulties in forward and reverse genetic investigations. To overcome this problem, selection of self-pollinating plants to obtain inbred homozygous plants is essential. Based on the head inflorescence and floret morphologies (Ferreira and Janick 1995), we hypothesize that self-pollinating plants can be obtained by hand pollination in optimized growth conditions. Accordingly, we have been trying to produce a set of homogenous, true breeding lines that will allow studying the genetics and biochemistry of artemisinin biosynthesis. From them, it is most likely to breed some lines that are useful for commercial production of artemisinin. Here, we report the establishment of a self-pollinated population of *A. annua* and the characterization of their morphology, development, and artemisinin biosynthesis under controlled growth conditions.

Materials and methods

Solvents and chemicals

Hydrochloric acid (36.5–38%, cat#: BHH3028-2.5L and ethyl acetate (cat#: BDH1123-19L) were purchased from BDH (West Chester, PA, 19380, USA). Acetonitrile (LC–MS grade) was purchased from EMD (cat#: AX0156-1, Gibbstown, NJ, 08027, USA). Acetic acid (HPLC grade, cat#: 9515-03) and methanol (LC–MS grade, cat#:

9830-03) were purchased from J. T. Baker (Phillipsburg, NJ, 08865, USA).

Medium preparation and seedling growth

Basal MS medium (Murashige and Skoog 1962) was used to geminate seeds and to grow seedlings. All media were adjusted to pH 5.8, solidified with phytoagar (0.6%) and then autoclaved for 20 min. Seeds were surface sterilized for 1 min with 70% ethanol and then treated with 10% Clorox 10 min followed by five times of wash with autoclaved water. Seed germination and seedling growth were carried out under light conditions of 16/8 h (light/dark) at 22–25°C.

Seeds and voucher specimen of *A. annua*

Seeds of *A. annua* L were kindly collected from the west bank of the Missouri River by Dr. George Yatskievych in the middle of October, 2006. The voucher specimen for our sample had been preserved in the Missouri Herbarium at the Missouri Botanical Garden. The label data for this voucher are as follows: "*Asteraceae-Artemisia annua* L. USA, Missouri, ST. Charles County, Katy Trail State Park, along the W bank of Missouri River under the Page Avenue Bridge; disturbed open sandy river terrace; plants common, up to 1.5 m tall, with *Symphyotrichum*, *Chenopodium*, *Ambrosia*, *Phyla*, grasses; 38°C 44′15.2″N Lat., 090°C 31′25.8″W long; T46N R04; elevation 430 ft. 22 October 2006 G. & K".

Plant growth in phytotron and greenhouse for seed production

Based on the short photoperiod of *A. annua* (Ferreira et al. 1995), plants were grown in two different growth conditions to test their seed production capability. Plants were grown in a phytotron. The phytotron protocol consisted of 13 days of growth in nursery bed under a 12-h photoperiod with a light intensity of 50 μmol m^{-2} s^{-1} and 19 days of growth in a controlled greenhouse with a 16-h photoperiod and temperatures of 26°C/22°C (day/night) followed by a short photoperiod of 8/16 h (light/dark) and the same temperature program in the phytotron. In detail, seeds were sown in a soil mixture consisting of peat-lite and sand (1:1) and geminated under a light intensity of 50 μmol m^{-2} s^{-1} and a 12-h photoperiod. During the light period, the pots were misted for 3 s per 3-min intervals and the temperature was set at 25°C. Seeds began geminating on day 3 after sowing and the seedlings were grown under the same conditions for an additional 10 days. On day 13, pots containing the seedlings were moved to an environmentally controlled greenhouse under ambient light conditions and

with a temperature program of 26°C/22°C (day/night). On day 32, seedlings that were approximately 3.5 cm tall with four or five leaves were transplanted to 10 cm (in diameter) pots filled with premier Pro-Mix-PGX (fine granulate) soil, one plant per pot, and then were transferred to a growth chamber with a photoperiod of 8/16 h (light/dark) and temperatures of 26°C/22°C (light/dark). Plants were watered in the morning with a nutrient solution and in the afternoon with deionized (DI) water each day (Saravitz et al. 2009).

Plants were grown in greenhouse. In the spring of 2007, seeds were sown in FAFARD 4P Mix soil contained in 15 cm (in diameter) pots, and germination was carried out in a regular greenhouse with a supply of natural light filtered by a glass roof. The temperature was ranged from 20°C (night time) to 35°C (day time). Pots were watered every day with tap water. Seeds began germinating after 3 days of the sown date, and plants were grown in a greenhouse.

Selection of self-pollinating plants in phytotron

To obtain a pedigree for our study, we called plants collected from Charles County as parent plants (Fig. 2). The second generation offspring plants were then obtained from the crossing of the parent plants grown in a phytotron (Fig. 2). These offspring plants that started the early development of raceme inflorescences were selected to test self-pollination (Fig. 2). Prior to the opening of the capitula, each plant was covered with a sleeve-like plastic bag (LEHLE SEEDS Cat. No SNS-01 ArabiSifter Floral Sleeves) with an opening in the top. After approximately 60 days, some individual plants that were approximately

25–30 cm in height began to flower. During the flowering period, in addition to daily watering and fertilizing as described above, plants were gently sprayed with DI water from above. After the start of inflorescence senescence, plants were no longer watered but were instead left to dry for approximately 2 weeks. When they were approximately 80 days old, dry inflorescences from the early-flowering plants were carefully collected and dry capitula were allowed to dry further for 2 days at room temperature, and then seeds were cleaned, kept in small paper bags, and stored at room temperature until use.

Seeds from the fast growth and early flowering plants were chosen for the continuous selection of the self-pollinating F1 plants (Fig. 2). Then, seeds from the F1-selfing plants with the earliest flowering times were used for the continuous selection of the F2 plants (Fig. 2). Selection of the F1 and F2 plants was performed in the same phytotron conditions as described above.

Optimization of growth conditions for flowering induction of F2 plants

As the protocol designed for seed germination and plant growth in the phytotron conditions described above, seeds produced by the self-pollinated F1 plants with the earliest flowering time were used to grow plants to further optimize growth conditions for early flowering induction. Thirty-two days after sowing, the seedlings (approximately 3.5 cm tall) were transplanted to Premier Pro-Mix-PGX (fine granulate) soil contained in 10 cm pots (in diameter), one plant per pot. After transplantation, the seedlings were transferred to a growth chamber with a short photoperiod of 8/16 h (light/ dark) and temperatures of 26°C in the daytime and 22°C in the night time. Plants were continuously grown for 10 days (until day 42). Forty-two-day-old plants were transferred to different growth conditions (Table 1; Fig. 3) to elongate their main stems and to induce flowering. The light intensity was set at 500–550 μmol m^{-2} s^{-1} in all growth chambers, and the light source was a cool white, florescent light. By following our phytotron protocol (Saravitz et al. 2009), all plants were watered in the morning with a nutrient solution and in the afternoon with deionized water each day. During plant growth, the numbers of leaves in the main stems and nodes starting to develop raceme inflorescences were recorded in detail.

Sample collection for characterization of trichomes, artemisinin biosynthesis, and gene expression in self-pollinated F2 plants

To characterize trichomes and artemisinin biosynthesis in these plants, a detailed sampling method from the F2 plants grown in the growth chamber is summarized in Table 2.
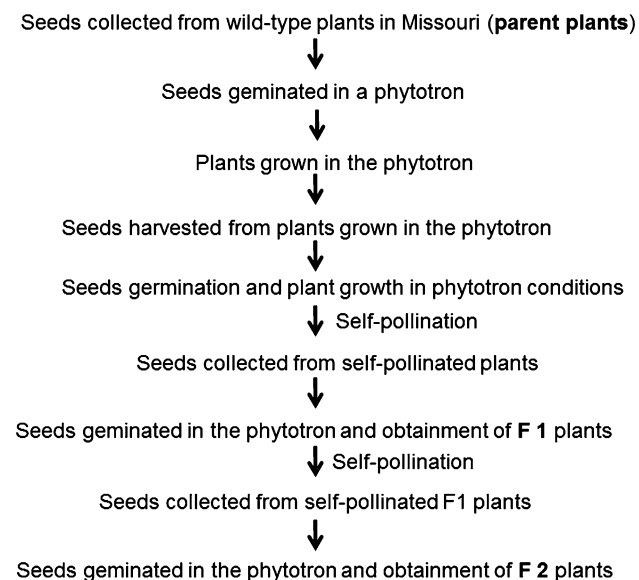
Seeds collected from wild-type plants in Missouri (**parent plants**)

↓

Seeds geminated in a phytotron

↓

Plants grown in the phytotron

↓

Seeds harvested from plants grown in the phytotron

↓

Seeds germination and plant growth in phytotron conditions

↓ Self-pollination

Seeds collected from self-pollinated plants

↓

Seeds geminated in the phytotron and obtainment of **F 1** plants

↓ Self-pollination

Seeds collected from self-pollinated F1 plants

↓

Seeds geminated in the phytotron and obtainment of **F 2** plants

Fig. 2 A schematic showing the self-pollination selection procedures of the plant population

Table 1 Five different growth conditions in phytotron were examined to induce early flowering of self-pollinated F2 plants after approximately 50 days of growth in 16/9 h (light/dark)

Conditions	Light/dark (h)	Temperatures (°C) (daytime/nighttime)	Flowering time (number of days after planting)
I	8/16	26/22	65
II	9/15	26/22	59
III	9/3+3/9 (L/D + L/D)	26/22	NF
IV	9/3+3/9 (L/D + L/D)	22/18	NF
V	9/15	22/18	NF

The flowering time was the number of days from the date of planting to the date of the first inflorescence formation

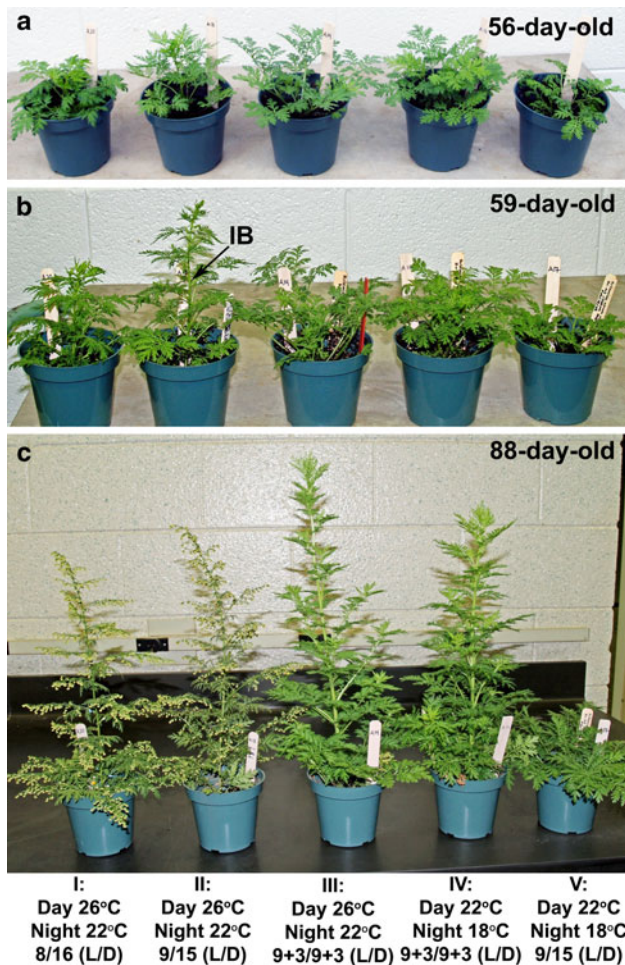*NF* no flower formation from plants grown in these conditions

Fig. 3 Effects of five different growth conditions on plant growth and heights, and flowering times. Before F2 plants were grown in these conditions, they were grown in the same conditions from seed germination until they were 42 days old (see "Materials and methods"). **a** Plants after 15 days of growth condition change; **b** plants after 18 days of growth condition change; **c** plants after 47 days of growth condition change

Scanning electron microscope and light microscope observation of trichomes in F2 plants

Leaves and inflorescences (Table 2) were trimmed to 2–3 mm^2 pieces when necessary. All samples were placed directly into a solution of cold 3% glutaraldehyde in 0.05 M pH 6.8 K_2HPO_4–KH_2PO_4 buffer and stored for approximately 2 weeks at 4°C. Samples were rinsed with the same buffer thrice with three 30-min changes and then dehydrated in a gradient of ethanol concentrations including 30, 50, 70, 95, and 100%. The treatment time is 1 hour for each concentration. The entire dehydration treatment was completed on ice. Samples were then warmed to room temperature, and dehydration was finally completed using two additional room temperature 100% ethanol changes. All samples were dried 15 min at critical point in liquid CO_2 (Tousimis Samdri-795, Tousimis Research Corporation, Rockville, MD, USA). Samples were mounted on stubs with double-stick tape, sputter coated with approximately 50Å of gold–palladium (Hummer 6.2 sputtering system, Anatech USA, Union City, CA, USA), and stored in a vacuum desiccator. Pollen samples were collected directly from the flowers, applied to double-stick tape, desiccated, and sputter coated as above. Samples were viewed at 15 kV using a JEOL JSM-5900LV (JEOL USA, Peabody, MA, USA).

The artemisinin biosynthesis was reported to localize in glandular trichomes on leaf surface (Duke et al. 1994). In our study, trichome densities on the surfaces of leaves (leaf #1 to 17) (Table 2) were estimated by obtaining counts from several 1 mm^2 areas with a light stereomicroscope. Four leaves from each node were collected from four individual plants and served as four replicates. Due to dramatic leaf morphology changes (called phase change) and size changes from leaf #1 to 17 (Fig. 3), to obtain unbiased trichome densities, the area size of leaf #1 was used as a standard for choosing lobed leaflets from leaves #4 to17 to count trichome numbers. The lobed leaflets (called

Table 2 Samples and sampling times were used for trichome profiling, artemisinin estimation, and RT-PCR analysis

Spatial positions of tissues	SEM analysis of trichomes	Trichome counting	Artemisinin analysis	RT-PCR analysis
Roots[a]			27-D-old S[a]	27-D-old S[a]
S[a]			27-D-old S[a]	27-D-old S[a]
Leaf #1	31-D-old S[b]	35-D-old S[b]	Pooled samples of leaves #1-6 of 43-D-old P[b]	Pooled samples of leaves #1-6 of 43-D-old P[b]
Leaf #2	31-D-old S[b]	35-D-old S[b]		
Leaf #3	31-D-old S[b]	35-D-old S[b]		
Leaf #4	31-D-old S[b]	35-D-old S[b]		
Leaf #5	31-D-old S[b]	35-D-old S[b]		
Leaf #6	31-D-old S[b]	35-D-old S[b]		
Leaf #7	66-D-old P	70-D-old P	73-D-old P	73-D-old P
Leaf #8	66-D-old P	70-D-old P	73-D-old P	
Leaf #9	66-D-old P	70-D-old P	73-D-old P	
Leaf #10	66-D-old P	70-D-old P	73-D-old P	73-D-old P
Leaf #11	66-D-old P	70-D-old P	73-D-old P	
Leaf #12	66-D-old P	70-D-old P	73-D-old P	
Leaf #13	52-D-old P	70-D-old P	73-D-old P	
Leaf #14	52-D-old P	70-D-old P	73-D-old P	73-D-old P
Leaf #15	52-D-old P	70-D-old P	73-D-old P	73-D-old P
Leaf #16	52-D-old P	70-D-old P	73-D-old P	73-D-old p
Leaf #17	52-D-old P	70-D-old P	73-D-old P	
Young racemes developed from the axillary buds of leaves #15, 16, and 17			73-D-old P	73-D-old P (only young racemes from leaves #15 and #16)
Unopened capitula	73-D-old P		73-D-old P	73-D-old P
Blooming capitula	73-D-old P		73-D-old P	73-D-old P

F2 seedlings were grown on agar-solidified MS medium to obtain roots and above-ground tissues. F2 plants grown in condition II were used for sampling tissues. The first true leaf after seed germination is defined as leaf #1 in our experiment, in turn, leaves #2, 3,… 17 in the main stems

D day, *P* plants, *S* seedlings

[a] These samples were harvested from seedlings grown on agar-solidified MS medium

[b] Leaves #1–6 were harvested from seedlings and plants grown in pots and pooled together as one sample

Area For Trichome counting, AFT) chosen from leaves #4 to 17 were those nearest to the main petioles (Fig. 4a). On each lobed leaflet, four different regions, representing the edge area, the tip area distant from the petiole, the middle area across the main vein, and the bottom area attached to the petiole on both adaxial and abaxial surfaces, respectively, were chosen to obtain the trichome numbers.

Extraction of artemisinin

Leaves, inflorescences, seedlings, and roots of F2 plants (Table 2) were chosen to analyze artemisinin. Leaves situated at the same nodal locations (from bottom to top) of the main stems from six individual plants were pooled together as one biological sample. Twenty-seven-day-old F2 seedlings grown on agar-solidified medium under long light conditions were harvested and then separated into roots and seedlings for artemisinin analysis. The fresh samples collected were immediately frozen in liquid nitrogen and stored at −80°C until use. Three biological replicates were prepared for each individual nodal leaf sample. Samples were homogenized into fine powder in liquid nitrogen with a mortar and pestle for the artemisinin extractions.

Next, 100 mg (fresh weight) of powder were extracted with 1 mL of ethyl acetate/acetonitrile (50:50) contained in a 1.5 mL Eppendorf tube. Each tube was vortexed vigorously and then sonicated for 10 min at room temperature followed by a 5 min centrifugation at a speed of 10,000 rpm. The supernatant was pipetted into a tube. The pellet was then suspended in 1 mL of the extraction solvent and this extraction step was repeated once. Subsequently, the two extracts were pooled together, and the solvent was dried off using nitrogen gas flow at room temperature. The residue remaining in the bottom of the tube was suspended in 200 μL of methanol. The methanol extract was then centrifuged at 13,000 rpm and 4°C to remove debris for the HPLC–MS analysis.

HPLC–ESI–MS analysis and determination of artemisinin

Artemisinin in samples was determined by high performance liquid chromatography–electrospray ionization–mass spectrometry analysis on a 2010 eV LC/UV/ESI/MS instrument (Shimadzu). An analytical reverse phase column, XDB-C18 (4.6 × 150 mm, diameter × length,
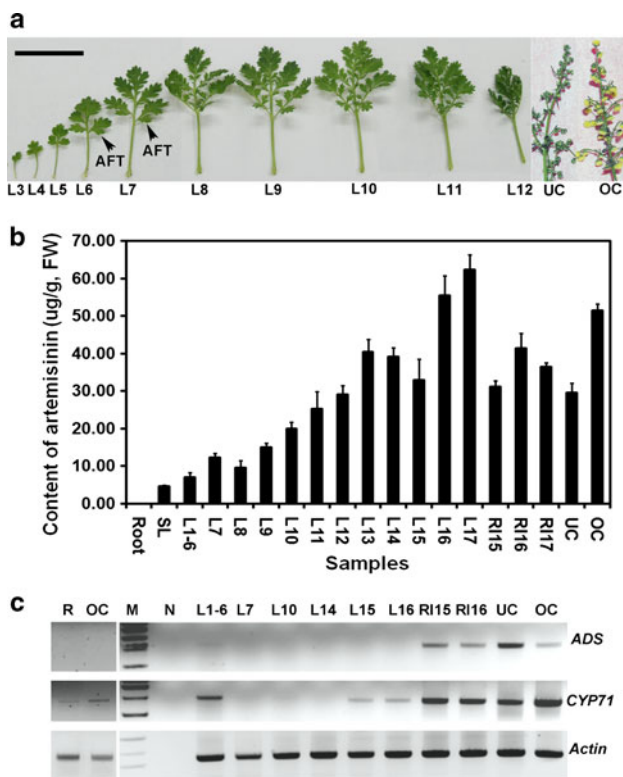
Fig. 4 Leaf morphologies, artemisinin content profiles, and RT-PCR analysis. **a** morphological features of leaves from leaves #3 through 12 on the main stems (arrows show locations of leaflets used for estimation of trichomes), AFT: area for trichome counting; **b** levels of artemisinin in leaves, young raceme inflorescence branches of the 15th, 16th, and 17th nodes of 73-day-old F2 plants, unopened capitula and opening capitula, 27-day-old seedlings excluding the roots, and roots (The artemisinin levels were a mean value estimated from three biological replicates. The *standard bars* were obtained from standard deviation of three replicates); **c** electrophoresis images show the intensities of RT-PCR fragment bands for *ADS*, *CYP71AV1*, and *ACTIN*. *L1-6* pooled samples of leaves #1 through 6 from 43-day-old seedlings; *L7, L8, L9, L10, L11, L12, L13, L14, L15, and L17* leaves #7 through 17 on the main stems of 73-day-old plants; *RI15, RI16, and RI17* young raceme inflorescence branches grown from the 15th, 16th, and 17th nodes of the main stems of 73-day-old plants; *UC* unopened capitula; *OC* opening capitula; *R* roots (from 27-day-old seedlings); *SL* seedling leaves (from 27-day-old seedlings); *N* negative control (Note: PCR analysis of root sample was completed at different times from PCR analyses of other samples)

5 μm, Agilent), was used to separate the samples. The mobile solvents included solvents A and B. Solvent A was 1% acetic acid in MS-grade water and solvent B was 100% methanol. Prior to sample separation, the column was equilibrated 30 min with a mixture solvent of A and B (80:20). The samples were separated with a gradient system that was composed of ratios of solvent A to B of 80:20 to 40:60 (0–5 min), 40:60 (5–30 min), 40:60 to 30:70 (30–32 min), 30:70 to 10:90 (32–34 min), and 10:90 to 80:20 (34–35 min). The gradient step was followed by a 10 min column wash with the mixture of solvent A and solvent B (80:20). The flow rate was set up at 0.6 mL/min

and the sample injection volume was 20 μl. The total ion chromatograms from the positive electrospray ionizations were recorded from 0 to 35 min by a mass spectrum detector, and the mass spectrum was scanned and stored from an *m/z* of 100 to 1,000 at a speed of 1,000 amu per second. Authentic standard artemisinin was used to obtain a standard curve for the estimations of artemisinin concentrations in samples. For quantification, we used ion chromatographic peak area values to estimate the levels of artemisinin.

RT-PCR analysis of *ADS* and *CYP71AV1*

Leaves, unopened and fully opened (blooming) capitula (Fig. 4a), seedlings without roots, and roots (Table 2) were analyzed to understand the expression patterns of *ADS* and *CYP71AV1*. After collection, samples were immediately frozen and ground into fine powder in liquid nitrogen; then 100 mg of powdered sample was used to isolate total RNA using the QIAGEN RNeasy Mini Kit according to the manufacturer's instructions. Total RNA was treated with RNase-free DNase I (Ambion, Foster City, CA, USA) at 37°C for 1 h to remove the residual genomic DNA, and the DNase was inactivated by phenol extraction. One microgram of treated RNA was subjected to first strand cDNA synthesis using the T-Primed First-Strand Kit (Amersham, Pittsburgh, PA, USA) according to the manufacturer's protocol. Primer pairs were designed based on *ADS* and *CYP71AV1* cDNA sequences (Table S1). In addition, specific *A. annua ACTIN* primer pairs were designed to amplify the *ACTIN* cDNA fragment as an internal standard (Table S1). One microliter of cDNA synthesis mixture was used as a template. The volume of each PCR reaction was 20 μl and 35 cycles were performed using the following program: 94°C for 1 min, 50°C (for *ACTIN*) or 56°C (for both *ADS* and *CYP71AV1*) for 30 s, 72°C for 1 (for *ACTIN*) or 2 (for both *ADS* and *CYP71AV1*) min. PCR products were examined with agarose gel electrophoresis.

Statistical analysis

A one way ANOVA and Student's *t* test were performed using StatCrunch (http://www.statcrunch.stat.ncsu.edu/) to evaluate the statistical significance ($P < 0.05$).

Results

Wild-type plant growth in the greenhouse and phytotron

A. annua plants grown in Charles County, Missouri were called parent plants in this study. Seeds were collected in

the fall of 2006. Approximately 80% of the seeds geminated in both the greenhouse and phytotron conditions (described in "Materials and methods"). In the greenhouse, most plants required 4–5 months to start flowering. In phytotron conditions, plants started to flower when they were approximately 60 days old. *A. annua* was able to flower and produce seeds in both the greenhouse and phytotron conditions. Given that the identities of the heterozygous plants were uncertain, in our experiment, we collected seeds from all individual plants and then stored them separately at room temperature until use.

Growth properties of F1 and F2 self-pollinating A. annua plants in phytotron

In this report, we only focused on selection of self-pollinating plants. We observed obvious segregations in the cross-pollinated offspring plants from the parent plants and characterized them by the following: fast-growing and slow-growing; early, late and no elongation of the main stem; and early, late, and no flowering. To reach the goal of this study, in our experiments, we only chose the fast-growing and early-flowering plants to test self-pollination so that the required time for selection of self-pollinating plants could be reduced. When the second generation offspring plants from the crossing of their parents (Fig. 2) were approximately 50 days old, certain numbers of them started to elongate their main stems and were covered with plastic bags. After approximately 60 days, some individual plants that were approximately 25–30 cm in height began to flower. When they were approximately 80 days old, dry inflorescences from the early-flowering plants were carefully collected for seed sorting. Seed yields from individual plants ranged from several mg to 1 g (approximately 10,000 seeds).

Segregations of the stem elongation times, flowering times, and plant heights in individuals were also observed in the F1 plant population. When the F1 plants were almost 60 days old, certain numbers of them started to flower. After approximately 80 days, the seeds were mature for collection and those seeds from the plants with the earliest flowering times were used for the continuous selection of the F2 population (Fig. 2).

Seeds (Fig. S1) collected from the F1 plants with the earliest flowering times were grown to select F2 plants. Most of the seeds geminated successfully under phytotron conditions. Segregations of stem elongation and flowering times in individuals were still observed in the F2 plants. Approximately, two-thirds of the F2 plants grew similarly in the pots (Fig. S2) and plants started to form raceme inflorescence branches around day 60 with seed maturation occurring at approximately 80 days.

Effects of five different growth conditions on flowering times of the F2 plants

Ninety-five F2 plants were grown in the same conditions for 46 days (see "Materials and methods"). Most were phenotypically similar, having similar leaf numbers and lengths of time for main stem elongation (Fig. S2). In our experiments, 80 morphologically similar plants (Fig. S2) were chosen to examine the effects of five separate conditions on growth (Table 1) and flowering time. Sixteen individual plants were grown in each condition. After approximately 2 weeks of growth in the different conditions, plants grown in condition II (9/15 h, light/dark) (Table 1) began to elongate their main stems (Fig. 3a). Under condition II, the approximately 60-day-old plants began to develop raceme inflorescence branches from their main stems (Fig. 3b; Table 1). In approximately 90 days, the seeds were mature for harvest (Fig. 3c). In comparison, the stem elongation time of plants, flowering time, and seed harvest times of the plants were 4–5 days late in condition I (8/16 h, dark/light) (Fig. 3a–c; Table 1). In addition, compared to condition II, plants grown in conditions III and IV began their stem elongation approximately 10 days later and did not flower. In condition V, plants did not show stem elongation but continued the initiation and growth of new rosette leaves (Fig. 3a–c). This experiment was repeated five times with the same results. Therefore, in our continuous experiments, we used condition II (Table 1) to grow the plants for morphological and phytochemical analyses.

Morphological changes of leaves and spatial characterization of inflorescence development in the F2 plants

F2 plants were grown under growth condition II to characterize their leaf morphologies and flowering times. The first true leaf that developed after seed germination was defined as leaf #1, the next as #2, #3, etc. Leaves #1–3 were single, lobed leaves with shallow indented margins (Fig. 4a). Leaf #4 is a single, lobed leaf with deeply indented margins (Fig. 4a). Leaf #5 was a trifoliate leaf, each leaflet of which had deeply indented margins (Fig. 4a). The terminal leaflet had three obvious lobes (Fig. 4a). Leaf #6 was an odd, pinnately compound leaf, with five lobed leaflets, each of which was only partially deeply indented in the margins (Fig. 4a). Leaf #7 was also an odd, pinnately compound with five lobed leaflets and deeply indented margins. Leaves #8–16 are odd and pinnately compound and had five leaflets that were completely or very deeply indented in the margins (Fig. 4a).

Most F2 plants grown in condition II developed their first complex raceme inflorescence, starting with the node

of the leaf #15, then leaf #16, etc. The number of inflorescence branches depended upon the individual plants. Each raceme inflorescence branch developed numerous capitula (Fig. 4a). After the formation of the first raceme branch, seeds were able to be harvested in 1 month. By the time of the seed harvest, the plants were 25–35 cm in height. This miniature property was beneficial to the inbred line selection experiments that took place in the growth chamber.

Trichome profiles

For approximately 20 years, investigations on artemisinin biosynthesis have focused on glandular trichomes (Covello et al. 2007; Duke et al. 1987; 1994; Ferreira and Janick 1995; Kim et al. 2008; Lommen et al. 2005; Ro et al. 2006; Tellez et al. 1999; Teoh et al. 2009; Wang et al. 2009). In our experiments, we used scanning electron microscopy (SEM) to examine the trichomes on the surfaces of the leaves, capitula, and flowers. Detailed SEM examinations showed glandular (consisting of 10 cells) and T-shaped trichomes on both the adaxial and abaxial surfaces of leaves #1–17 (Fig. 5a–f) and the surfaces of the involucres, petals, and florets (Fig. 6a–d) as reported previously for field-grown plants (Duke et al. 1994; Ferreira and Janick 1995).

The densities of the glandular trichomes were estimated for leaves #1–17 (Table 2). Leaves #1–6 were collected at the same time from 35-day-old seedlings, when the expansion of these leaves had stopped. Leaves #7–17 were carefully collected from 70-day-old plants at the same time. The densities for the total glandular trichomes from adaxial and abaxial surfaces were higher ($14–42/mm^2$) on leaves #7–17 than on leaves #1–6 ($5–9/mm^2$) (Fig. 7a). The glandular trichome densities on the two surfaces of the leaves were dependent upon each individual leaf.

In addition, the densities of the T-shaped trichomes were estimated for leaves #1–17. Although T-shaped trichomes were formed in all leaves examined, we did not observe a density trend for this type of trichome on both surfaces of the leaves (Fig. 7b).

Characterization of flowers in F2 plants

Each capitulum produced two types of florets, hermaphroditic and pistillate (Fig. 6d). Before the opening of the capitula, florets were wrapped completely by imbricate bracts (Fig. 6a). Disc florets were hermaphroditic, while ray florets were pistillate (Fig. 6c). Mature and functional pollens were triporate (Fig. 6e, f).

HPLC–MS analysis of artemisinin

We used HPLC–ESI–MS to analyze artemisinin in samples, including the following: seedlings without roots, pooled
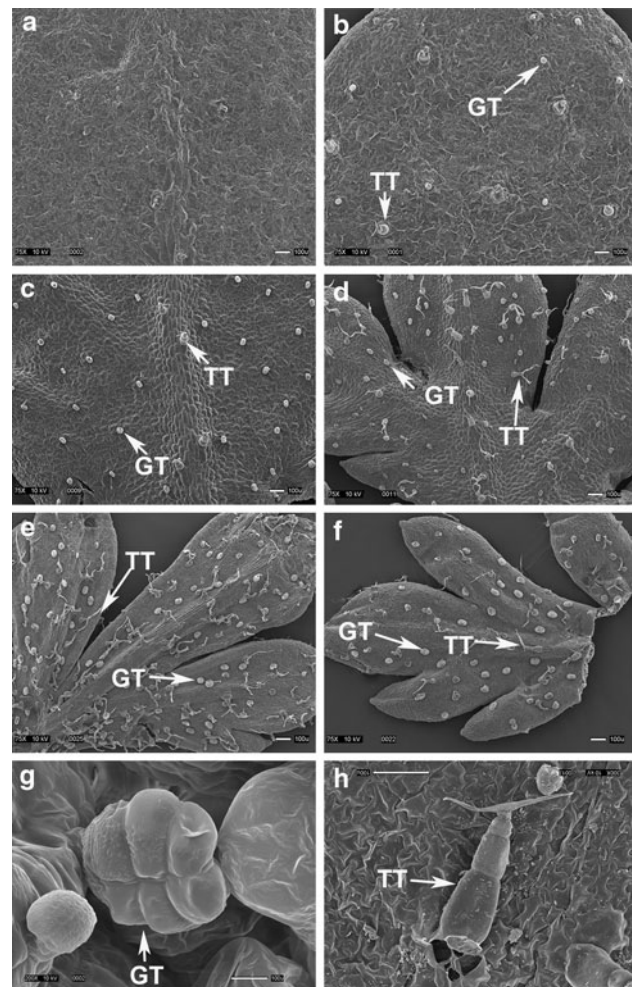

Fig. 5 Images of electron scanning microscopy, showing trichomes on the surfaces of leaves. Abaxial (**a**) and adaxial (**b**) surfaces of leaf #1; abaxial (**c**) and adaxial (**d**) surfaces of leaf #7; abaxial (**e**) and adaxial (**f**) surfaces of leaf #17; magnified images of glandular (**g**) and T-shaped (**h**) trichomes. *GT* glandular trichome; *TT* T-shaped trichome

leaves #1–6 from 43-day-old plants, individual leaves #7–17 from 73-day-old plants; raceme inflorescence branches with unopened capitula developed from the axillary buds of leaves #15, 16, and 17, unopened capitula and opening capitula, and roots (Table 2). With the exception of the root, artemisinin was observed in all samples (Fig. 4b, Fig. 8). Two main mass fragments from the artemisinin standard were detected by positive ionization, $341[m/z]^+ = [QHS+Na+Cl]^+$ and $305 [m/z]^+ = [QHS+Na]^+$ (Fig. 8). The artemisinin produced by the samples showed the same mass spectrum profiles (Fig. 8).

The levels of artemisinin in the samples were estimated by the use of the peak area values from the total ion chromatography based on a standard curve for artemisinin. In the leaf samples analyzed, in general, the levels of artemisinin showed an increasing trend from leaf #8 to leaf

#17 (Fig. 4b), including three specific trends: a significant increase from leaf #8 to leaf #13 ($p < 0.05$), similar levels from leaf #13 to leaf #15, and a significant increase from leaf #15 to leaf #16 ($p < 0.05$). The levels of artemisinin were similar between leaf #16 and leaf #17. The levels of
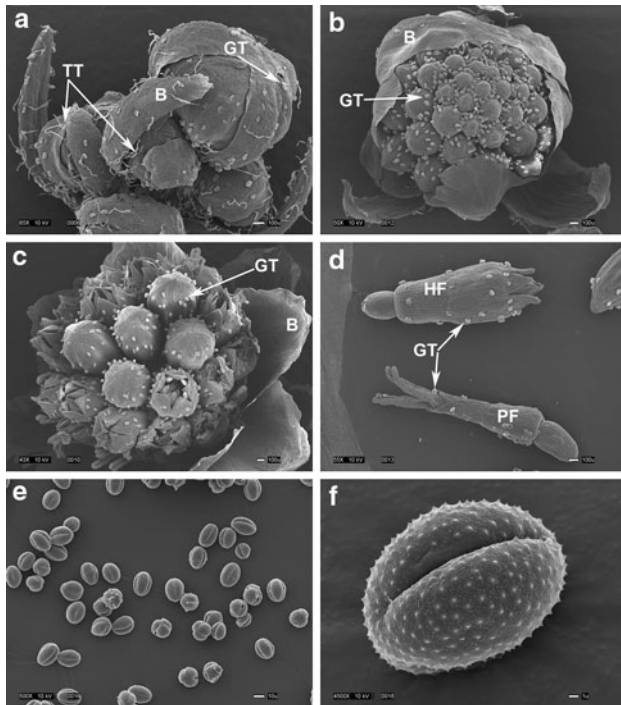
artemisinin in the pooled leaves #1–6, leaf #7, and leaf #8 were similar but significantly higher than in the seedlings (Fig. 4b). There was a positive correlation between the levels of artemisinin in leaves (Fig. 4 b) and the densities of total glandular trichomes on leaf surfaces (including both adaxial and abaxial sides) (Fig. 7a). Our observation supports that glandular trichomes likely are the artemisinin formation location reported previously (Duke et al. 1994). Opening capitula produced higher levels of artemisinin ($p < 0.05$) than unopened capitula and young inflorescence branches but less than leaves # 16 and #17 (Fig. 4b). A one-way ANOVA analysis did not show significant differences among leaves #13–15, young inflorescence branches #15–17, and unopened capitula. No artemisinin was detected in the roots (Fig. 8).

Expression patterns of *ADS* and *CYP71AV1*

ADS (Fig. 1) has been enzymatically and transgenically demonstrated to convert FPP to amorpha-4, 11-diene, the essential committed step in artemisinin biosynthesis and its cDNA was cloned from glandular trichomes (Bouwmeester et al. 1999; Chang et al. 2000; Martin et al. 2003; Mercke et al. 2000; Ro et al. 2006; Wallaart et al. 2001; Zhang et al. 2010). *CYP71AV1* (Fig. 1), a P450 enzyme coupled with a CPR, has been demonstrated to catalyze a three-step reaction, converting amorpha-4, 11-diene to artemisinic acid in transgenic yeast, and its cDNA was also cloned from glandular trichomes (Ro et al. 2006; Teoh et al. 2006). RT-PCR analyses were carried out to evaluate the transcripts of *ADS* and *CYP71AV1* in the leaves and flowers. Leaf samples analyzed included pooled leaves #1-6 from 43-day-old plants, leaf #7, leaf # 10, and leaves #14–16 from 73-day-old plants (Table 2). Young raceme inflorescence branches included the ones developed from
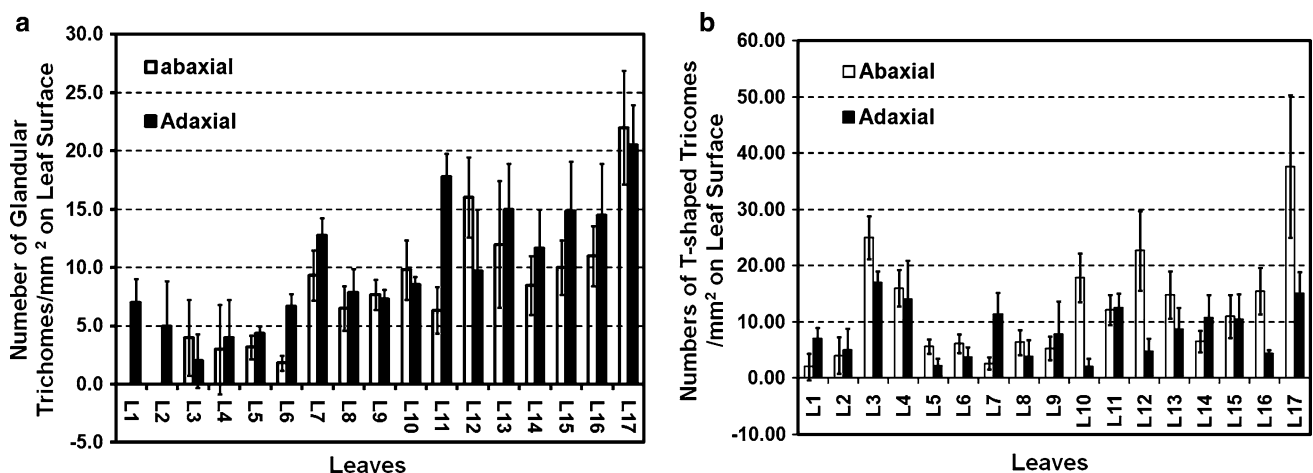

Fig. 6 Images of electron scanning microscopy, showing unopened capitula, opening capitula, trichomes, florets, pollen, and imbrication of bracts. **a** Unopened capitula; **b** an almost half-opened capitulum and floret buds; **c** a fully opened capitulum, floret buds, and opening florets; **d** a hermaphroditic floret and a pistillate floret; **e** mature pollens; **f** a magnified mature pollen. *B* bract, *HF* hermaphroditic floret, *PF* pistillate floret, *GT* glandular trichome, *TT* T-shaped trichome

Fig. 7 Estimation of glandular (**a**) and T-shaped (**b**) trichome densities on both adaxial and abaxial surfaces of leaves; *L1–6* leaves #1 through 6 from 35-day-old seedlings; *L7–17* leaves #7 through 17 on the main stems of 70-day-old plants
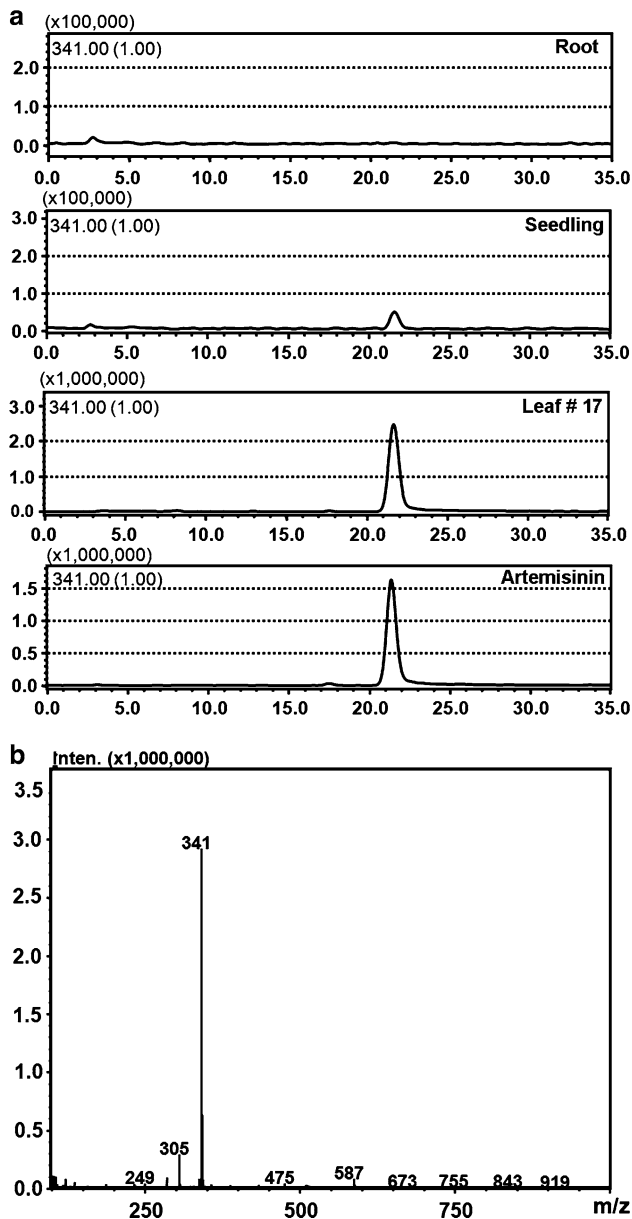
Fig. 8 LC–MS analysis, showing artemisinin produced in the leaves and seedlings. **a** total ion chromatograph profiles show that leaf #17 and seedlings but not roots produced artemisinin detected at the same retention time as the authentic standard; **b** the major MS fragment of artemisinin (for both standard and sample extracts) ionized by positive electron spray is at 341 $[m/z]^+$

leaves #15 and #16 (Table 2). Flower samples included unopened and opening capitula. The transcript of *ADS* was observed in unopened capitula, opening capitula, young raceme inflorescence branches #15–16, and the pooled leaves #1–6, with cDNA fragment band representing the unopened capitulum showing the highest intensity (Fig. 4c). However, the transcript of *ADS* was neither observed in leaves #7, #10, and #14–16 nor the roots (Fig. 4c). The transcript of *CYP71AV1* was observed in the pooled leaves #1–6, leaves #15–16, inflorescence branches,

and unopened and opening capitula (Fig. 4c), among which the cDNA fragment band from the opening capitula showed the highest intensity, and the ones from leaves #15 and #16 showed the lowest intensity (Fig. 4c). However, the transcript of *CYP71AV1* was not detected in leaves #7, #10, and #14 (Fig. 4c). It was very interesting that the transcript of *CYP71AV1* was detected in the roots of the seedlings (Fig. 4c).

Discussion

Peter-Blanc et al. (1992) reported that it was difficult for the flowers of *A. annua* to self-pollinate if they were covered in bags. More studies have shown that *A. annua* favors cross-hybridization in nature (Delabays et al. 2001). The mechanism of this difficult self-pollination in *A. annua* has remained unclear. Based on floret morphologies (Ferreira and Janick 1995), we hypothesize that self-pollination can be achieved in controlled growth conditions. When we began our growth chamber experiments, we focused on flowering time and flower structures. As reported by Ferreira and Janick (1995), plants grown in growth chambers formed hermaphroditic florets (disc flowers) and pistillate florets (ray flowers) (Fig. 6b–d). The order of floret opening in the capitula is from ray to disc florets (Fig. 6c). In our experiments, due to the miniature properties (35–35 cm) of the plants grown in pots, we covered the entire plants with sleeve-like plastic bags with open tops for the self-pollination. This approach allowed flowers to be exposed to light, and every plant produced seeds. For the pollination of pistillate florets, the pollen must be transported from the hermaphroditic florets. For the pollination of hermaphroditic florets, whether pollen was from the plants' own anthers or other florets in the same plant remains unknown. Consequently, each self-pollinated plant line obtained in our experiment resulted from one parent plant.

As described in the introduction, the goal of this study was to develop self-pollinating plants to study artemisinin biosynthesis. Particularly, self-pollination *A. annua* plants are suitable for functional genomics studies. These plants grown in the growth chamber had relatively short (90 days) life cycles, produced appropriate yields of seeds, developed glandular trichomes, and produced artemisinin. In addition, their miniature sizes were similar to *Arabidopsis thaliana* in height. These properties allow the plants to be grown in growth chamber, which facilitates the convenience of performing various experiments, e.g., mutagenesis and the selection of mutants. Molecular and biochemical studies have identified several genes involved in the formation of artemisinin precursors (Covello et al. 2007; Liu et al. 2006; Weathers et al. 2006). Particularly, two key pathway genes, *ADS* and *CYP71AV1*, were cloned and demonstrated to be

involved in the formation of artemisinic acid (Covello et al. 2007; Ro et al. 2006; Teoh et al. 2006; Weathers et al. 2006). To our knowledge, knock-out mutant lines of these two genes or transgenic studies of them in *A. annua* are lacking. Therefore, their roles in artemisinin biosynthesis in *A. annua* remain to be elucidated. We expect that the self-pollinating *A. annua* plants may be used as a model organism to help overcome this problem by allowing the knockout of these genes and others involved in artemisinin biosynthesis. We have obtained multiple individual F2 lines that express *ADS* and *CYP71AV1* genes (Fig. 4c) and produce artemisinin (Fig. 8). To date, we have obtained F5 seeds. We expect to use their offspring plants for mutagenesis experiments to develop mutant lines, including both cloned and unknown genes, to greater understand the biosynthesis and genetic regulation of artemisinin. In addition, we expect to obtain inbred homozygous plants for the genetic breeding of *A. annua* to overcome the low and variable artemisinin production problem. Another potential use of self-pollinating plants is as model plants of Asteraceae (sunflower) family, the largest dicotyledonous family.

The expression patterns of *ADS* and *CYP71AV1* in plants have not yet been investigated. In our experiment, artemisinin was produced in all leaf samples (Fig. 4b); however, the expression of *ADS* was not detected in five leaf samples examined (Fig. 4c), and the *CYP71AV1* transcript was only detected in leaves #15 and 16 as well as pooled samples of leaves #1–6. These PCR results were likely due to the ages of the leaves when they were collected. We sampled leaves #7, 10, 14, 15 and 16 at the same time from 73-day-old plants for the RT-PCR analysis. Among these samples, leaf #16 was the youngest tissue, followed by leaves #15, 14, 10 and 7. These age differences may explain that the *CYP71AV1* transcript was only detected in leaves #15 and 16 but not in leaves #7 and 10 by RT-PCR analysis. It was interesting that the transcript of *ADS* was not detectable in leaves #15 and 16. This observation suggests that *ADS* was expressed at a very early stage of leaf development. This was further demonstrated by our recent cloning of the cDNAs of the two genes from very young samples of leaf #7. As expected, the expression of *ADS* was not detected in the roots (Fig. 4c). This may explain why the roots did not produce artemisinin (Fig. 8). In contrast, the expression of *CYP71AV1* was clearly detected in the roots, suggesting that CYP71AV1 is involved in other biochemical processes in roots.

References

Acton N, Klayman DL (1985) Artemisitene, a new sesquiterpene lactone endoperoxide from *Artemisia annua*. Planta Med 51:441–442

Bouwmeester HJ, Wallaart TE, Janssen MHA, van Loo B, Jansen BJM, Posthumus MA, Schmidt CO, De Kraker J-W, Konig WA, Franssen MCR (1999) Amorpha-4, 11-diene synthase catalyses the first probable step in artemisinin biosynthesis. Phytochemistry 52:843–854

Chang Y-J, Song S-H, Park S-H, Kim S-U (2000) Amorpha-4, 11-diene synthase of *Artemisia annua*: cDNA isolation and bacterial expression of a terpene synthase Involved in artemisinin biosynthesis. Arch Biochem Biophys 383:178–184

Covello PS, Teoh KH, Polichuk DR, Reed DW, Nowak G (2007) Functional genomics and the biosynthesis of artemisinin. Phytochemistry 68:1864–1971

Delabays N, Benakis A, Collet G (1993) Selection and breeding for high artemisinin (qinghaosu) yielding strains of *Artemisia annua*. Acta Horticult 330:203–207

Delabays N, Simonnet X, Gaudin M (2001) The genetics of artemisinin content in *Artemisia annua* L. and the breeding of high yielding cultivars. Curr Med Chem 8:1795–1801

Duke SO, Vaughn KC, Croom EM Jr, Elsohly HN (1987) Artemisinin, a constituent of annual wormwood (*Artemisia annua*), is a selective phytotoxin. Weed Sci 35:499–505

Duke MV, Paul RN, Elsohly HN, Sturtz G, Duke SO (1994) Localization of artemisinin and artemisitene in foliar tissues of glanded and glandless biotypes of *Artemisia annua* L. Int J Plant Sci 155:365–372

Ferreira JFS, Janick J (1995) Floral morphology of *Artemisia annua* with special reference to trichomes. Int J Plant Sci 156:807–815

Ferreira JFS, Simon JE, Janick J (1995) Developmental studies of *Artemisia annua*: Flowering and artemisinin production under greenhouse and field conditions. Planta Med 61:167–170

Ferreira JFS, Laughlin JC, Delabays N, Magalhães PMd (2005) Cultivation and genetics of *Artemisia annua* L. for increased production of the antimalarial artemisinin. In: Koebner R (ed) Plant Genetic Resources. Cambridge University Press, Cambridge, pp 206–229

Graham IA, Besser K, Blumer S, Branigan CA, Czechowski T, Elias L, Guterman I, Harvey D, Isaac PG, Khan AM, Larson TR, Li Y, Pawson T, Penfield T, Rae AM, Rathbone DA, Reid S, Ross J, Smallwood MF, Segura V, Townsend T, Vyas D, Winzer T, Bowles D (2010) The genetic map of *Artemisia annua* L. identifies loci affecting yield of the antimalarial drug artemisinin. Science 327:328–331

Kim S-H, Chang Y-J, Kim S-U (2008) Tissue specificity and developmental pattern of amorpha-4, 11-diene synthase (ADS) proved by ADS promoter-driven GUS expression in the heterologous plant, *Arabidopsis thaliana*. Planta Med 74:188–193

Klayman DL, Lin AJ, Acton N, Scovill JP, Hoch JM, Milhous WK, Theoharides AD, Dobek AS (1984) Isolation of artemisinin (Qinghaosu) from *Artemisia annua* growing in the United States. J Nat Prod 47:715–717

Liersch R, Soicke H, Stehr C, Tüllner H-U (1986) Formation of artemisinin in *Artemisia annua* during one vegetation period. Planta Med 52:387–390

Liu J-M, Ni M-Y, Fan J-F, Tu Y-Y, Wu Z-H, Wu Y-L, Chou W-S (1979) Structure and reaction of arteannuin. Acta Chim Sin 37:129–143

Liu C, Zhao Y, Wang Y (2006) Artemisinin: current state and perspectives for biotechnological production of an antimalarial drug. Appl Microbiol Biotechnol 72:11–20

Lommen WJ, Schenk E, Bouwmeester HJ, Verstappen FW (2005) Trichome dynamics and artemisinin accumulation during

development and senescence of *Artemisia annua* leaves. Planta Med 71:336

Lommen WJM, Elzinga S, Verstappen FWA, Bouwmeester HJ (2007) Artemisinin and sesquiterpene precursors in dead and green leaves of *Artemisia annua* L. crops. Planta Med 73:1133–1139

Martin VJJ, Pitera DJ, Withers ST, Newman JD, Keasling JD (2003) Engineering a mevalonate pathway in *Escherichia coli* for production of terpenoids. Nat Biotech 21:796–802

Mercke P, Bengtsson M, Bouwmeester HJ, Posthumus MA, Brodelius PE (2000) Molecular cloning, expression, and characterization of amorpha-4, 11-diene synthase, a key enzyme of artemisinin biosynthesis in *Artemisia annua* L. Arch Biochem Biophys 381:173–180

Murashige T, Skoog F (1962) A revised medium for rapid growth and bioassays with tobacco tissue culture. Physiol Plant 15:473–497

Peter-Blanc C (1992) Developpement et biologie de la reproduction de l'*Artemisia annua* L. Travail de diplome. Université de Lausanne, Suisse

Ro D-K, Paradise EM, Ouellet M, Fisher KJ, Newman KL, Ndungu JM, Ho KA, Eachus RA, Ham TS, Kirby J, Chang MCY, Withers ST, Shiba Y, Sarpong R, Keasling JD (2006) Production of the antimalarial drug precursor artemisinic acid in engineered yeast. Nature 440:940–943

Saravitz CH, Downs RJ, Thomas JF (2009) PHYTOTRON PROCE-DURAL MANUAL: For Controlled-Environment Research at the Southeastern Plant Environment Laboratory. http://www.ncsu.edu/phytotron/manual.pdf

Smith LMJ, Bentley S, Jones H, Burns C, Arroo RRJ, Woolley JG (2010) Developing an alternative UK industrial crop *Artemisia annua*, for the extraction of artemisinin to treat multi-drug resistant malaria. Asp Appl Biol 101:99–106

Tellez MR, Canel C, Rimando AM, Duke SO (1999) Differential accumulation of isoprenoids in glanded and glandless *Artemisia annua* L. Phytochemistry 52:1035–1040

Teoh KH, Polichuk DR, Reed DW, Nowak G, Covello PS (2006) *Artemisia annua* L. (*Asteraceae*) trichome-specific cDNAs reveal CYP71AV1, a cytochrome P450 with a key role in the biosynthesis of the antimalarial sesquiterpene lactone artemisi-nin. FEBS Lett 580:1411–1416

Teoh KH, Polichuk DR, Reed DW, Covello PS (2009) Molecular cloning of an aldehyde dehydrogenase implicated in artemisinin biosynthesis in *Artemisia annua*. Botany 87:635–642

Tu Y-y, Ni M-y, Zhong Y-r, Li L-n, Cui S-l, Zhang M-q, Wang X-z, Ji Z, Xiao-tian L (1982) Studies on the constituents of *Artemisia annua* Part II. Planta Med 44:114–143

Wallaart TE, Pras N, Quax WJ (1999) Seasonal variations of artemisinin and its biosynthetic precursors in tetraploid *Artemisia annua* plants compared with the diploid wild-type. Planta Med 65:723–728

Wallaart TE, Pras N, Beekman AC, Quax WJ (2000) Seasonal variation of artemisinin and its biosynthetic precursors in plants of *Artemisia annua* of different geographical origin: proof for the existence of chemotypes. Planta Med 66:57–62

Wallaart TE, Bouwmeester HJ, Hille J, Poppinga L, Maijers NCA (2001) Amorpha-4, 11-diene synthase: cloning and functional expression of a key enzyme in the biosynthetic pathway of the novel antimalarial drug artemisinin. Planta 212:460–465

Wang W, Wang Y, Zhang Q, Qi Y, Guo D (2009) Global characterization of *Artemisia annua* glandular trichome transcriptome using 454 pyrosequencing. BMC Genomics 10:465

Weathers P, Elkholy S, Wobbe K (2006) Artemisinin: The biosynthetic pathway and its regulation in *Artemisia annua*, a terpenoid-rich species. In Vitro Cell Dev Biol Plant 42:309

WHO (1998) Artemisinin and its derivatives as anti-malarial drugs. Artemisinin and its Derivatives as Anti-Malarial Drugs, Geneva

WHO (2005) Meeting on the production of artemisinin and artemis-inin-based combination therapies, 6–7 June 2005, Arusha, United Republic Tanzania

WHO (2009a) Impact of malaria control. World Malaria Report 2009, Geneva, pp 27–44

WHO (2009b) Interventions to control malaria. World Malaria Report 2009. World Health Organization, Geneva, pp 9–26

WHO (2009c) Polices, stratagies adn targets for malaria control. World Malaria Report 2009, Geneva

WHO (2010) Good procurement practices for artemisinin-based antimalarial medicines. WHO Global Malaria Programme

Xie D-Y, Kang N-l, Li G-z (1995) Studies on the karyotype of *Artemisia annua*. Chin Bull Botany 12(Supplement):71–72

Zhang Y, Teoh KH, Reed DW, Maes L, Goossens A, Olson DJH, Ross ARS, Covello PS (2008) The molecular cloning of artemisinic aldehyde u11(13) reductase and its role in glandular trichome-dependent biosynthesis of artemisinin in *Artemisia annua*. J Biol Chem 283:21501–21508

Zhang Y, Nowak G, Reed DW, Covello PS (2010) The production of artemisinin precursors in tobacco. Plant Biotechnol J. doi:10.1111/j.1467-7652.2010.00556.x (in press)

Zhong-Yi-Yan-Jiu-Yue-Zhong-Yao-Yan-Jiu-Suo (1978) Qing Hao Kang Nue Yan Jiu:1971-1978 (Antimalarial studies of *Artemisia annua* L:1971–1978). Zhong Yi Yan Jiu Yue Zhong Yao Yan Jiu Suo